Analysis of subgrid scale phenomena of premixed turbulent combustion of methane and hydrogen in comparable regimes

By R. J. M. Bastiaans AND M. S. Day

1. Motivation and objectives

Computational simulation of turbulent combustion has the potential to play a very important role in fundamental research and in the design of combustion devices, yet it remains problematic for many practical applications. Although it is certainly possible to perform fully resolved direct numerical simulations (DNS) with detailed chemistry and transport on idealized centimeter-scale domains, even these "toy" applications require massive computing resources. For the study of practical devices, the huge disparity in spatial and temporal scales renders such studies infeasible now and for the foreseeable future.

A more manageable approach to simulating combustion devices at the device scale can be developed by dramatically reducing the degrees of freedom used to represent the solution. Reynolds Averaged Navier Stokes (RANS) methods, for example, replace the detailed model with one based on a set of time-averaged variables. Since fastest time scales are no longer evolved in this reduced system explicitly, their effects on the resolved scales, if significant, must be incorporated through explicit models. Similarly, Large Eddy Simulation (LES) methods are based on a spatial filtering of the equations that eliminates small length scales. Unfortunately, most combustion processes of interest involve coupling across these scales, and the coupling is both strong and highly nonlinear. Modeling terms are essential to adequately account for subgrid processes on the resolved fields.

The goal of the present work is to explore the applicability of yet another reduction approach, the presumed probability density function (PDF) method. Presumed PDF methods are based on the use of an efficient representation for flow or thermodynamic variable distributions (or joint distributions) that use parameterized functional forms. We consider the β-PDF form in particular, and explore its utility to capture key aspects of a class of turbulent premixed lean combustion problems by evaluating actual distributions taken from numerically resolved DNS solutions.

The β-PDF (reviewed in more detail in Section 2) can be used to parameterize the distribution of a variety of scalar fields in reacting flow problems. Candidate fields are typically bounded on physical grounds to values arbitrarily between 0 and 1. For example, early combustion-related applications of β-PDF methods include the work by Cook & Riley (2004), where the β-PDF was used to represent the mixture fraction field in a diffusion flame configuration. In premixed flames, a natural candidate to use is "reaction progress", a scalar which rises from 0 in the cold fuel to 1 in the hot products. Any scalar field that monotonically increases through the flame front can potentially serve as a valid progress variable. For example, in lean methane flames with low levels of turbulence, both the temperature and fuel content are frequently inter-changeable as valid progress variables. In flames with significant differential or preferential transport effects,

the identification of a comparable scalar field that can serve as an unambiguous progress variable may not be as clear. For example, unstrained lean premixed hydrogen fuels burn in multidimensional cellular flame structures, and the gradients of temperature and fuel concentration through the flame zone are not co-linear. Clearly then, the behavior of a PDF scheme will be impacted by how the reaction progress is defined in these cases.

In this paper, we explore whether a lean premixed turbulent hydrogen-air flame can be well-represented by a β-PDF approach as traditionally applied. Given the increasing importance of premixed hydrogen-air and hydrogen-seeded methane-air flames as potential fuels for low-emissions combustion systems, we seek to evaluate the prospects of this approach to studying premixed hydrogen-air systems.

We begin with a suite of pre-computed DNS simulations of a turbulent, statistically one-dimensional flame brush. The configuration is a high aspect ratio three-dimensional box that is periodic in the directions orthogonal to the mean flame propagation. The bottom boundary is an adiabatic free slip wall, and hot combustion products flow freely out of the domain top. We are interested in lean hydrogen-air mixtures, and use similar systems fueled with lean methane-air mixtures as "control" cases in order to highlight specific features of the hydrogen systems. Turbulence in the DNS configurations is maintained by imposing a time-dependent large-scale forcing term (stirring) that generates a Kolmogorov spectrum of fluctuation scales. The integral length scale of the resulting turbulence is determined by the box dimensions in the transverse (periodic) directions, and the intensity is governed by the magnitude of externally applied force. We posit that the time-dependent DNS solutions represent the full dynamics of the system for analysis. Statistics are gathered from the simulated flame by first defining a mean progress field (averaging the selected progress field in the periodic direction), and then defining "fluctuations" in any such plane as the local deviations from this mean.

We consider a progress variable for turbulent premixed flames that is defined in the framework of flamelet generated manifolds (FGM) as in van Oijen & de Goey (2000), Gicquel et al. (2000), Vreman et al. (2009) and, particularly in the context of hydrogen addition to premixed methane-air fuels, see de Swart et al. (2010). Although the FGM approach is typically combined with a DNS model for the flow field, it can also be incorporated naturally into LES and RANS models to reduce computing requirements associated specifically with the high-dimensional chemical composition space. We evaluate PDFs from the DNS database and compare them with those of the standard β-PDF forms, with the ultimate goal of validating a PDF-based model for use in an LES simulation framework. We will show that the β-PDF model is a remarkably effective reduction approach in the methane case, where reaction progress can be unambiguously mapped to a valid progress variable. However, we also show that the model is less useful for systems that exhibit a more ambiguous multidimensional notion of reaction progress.

Note that the approach for constructing the diagnostics used in this study tacitly assumes that the horizontal mean temperature profile represents a viable measure of mean progress. An area of future study is whether our conclusions are essentially independent of the choice between "reasonable" progress measures (and whether, in fact, such a quantity exists). Additionally, the approach assumes that the finite extent of the DNS solution domain is sufficiently large that horizontal averages yield statistically converged (and 1D) diagnostics. Although some of the issues involved in making this latter determination are discussed in the references, this too is an area that merits more explicit confirmation in follow-on investigations.

The paper is organized as follows: Section 2 provides a review of the basic properties

$\mu(x)$	$\sigma(x)$	$\gamma(x)$	$\alpha(x)$	$\beta(x)$
1/2	1/5	1/4	1/8	1/8
1/2	1/12	2	1	1
1/2	1/20	4	2	2
1/2	1/25	15/4	21/8	21/8
2/7	10/392	7	2	5
1/4	3/80	4	1	3
5/6	5/252	6	5	1

TABLE 1. Values for γ, α and β as function of selected means and variances of x.

of the β-PDF functional form. Section 3 reviews the configuration and simulation details used to generate the DNS database. Section 4 presents a summary of the actual DNS data. Section 5 presents PDFs of the DNS data with respect to the β-PDF functional forms for both the methane and hydrogen flame sets. Section 6 discusses several additional considerations specifically associated with the lean hydrogen flames. Finally, in Section 7 we summarize the main conclusions and suggest directions for related future work along these lines.

2. The β-pdf distribution

The probability density function of the beta distribution of a function $f(x)$ with mean of x being μ and the variance being σ, or shorthand the β-pdf, is given by

$$f(x,\mu,\sigma) = f(x,\alpha,\beta) = \frac{x^{(\alpha-1)}(1-x)^{(\beta-1)}}{B(\alpha,\beta)}, \tag{2.1}$$

calculating α and β from the mean and variance by

$$\alpha = \mu\gamma \qquad \beta = (1-\mu)\gamma \qquad \gamma = \frac{\mu(1-\mu)}{\sigma} - 1, \tag{2.2}$$

and

$$B(\alpha,\beta) = \frac{\Gamma(\alpha+\beta)}{\Gamma(\alpha)+\Gamma(\beta)}. \tag{2.3}$$

B is the beta function and the gamma function $\Gamma(z)$ is used. For σ approaching 1/4, Equation 2.1 simplifies to a double δ distribution with the mean determining the symmetry. And at symmetry with $\sigma = 1/12$ the uniform distribution is obtained. At smaller variances, $\sigma \approx 1/25$, the gradient at the maxima approaches 0 very fast and the distribution becomes Gaussian; for very small values it approaches a single delta peak.

3. DNS simulations

The currently analyzed DNS data are for the case of statistically 1D turbulent premixed combustion in the thin reactions regime (TRZ), see Peters (2000). Methane and hydrogen cases are considered for which the equivalence ratio was such that the Karlovitz numbers, specified by the sequence Ka=1, 4, 12 and 36, were comparable. The Karlovitz

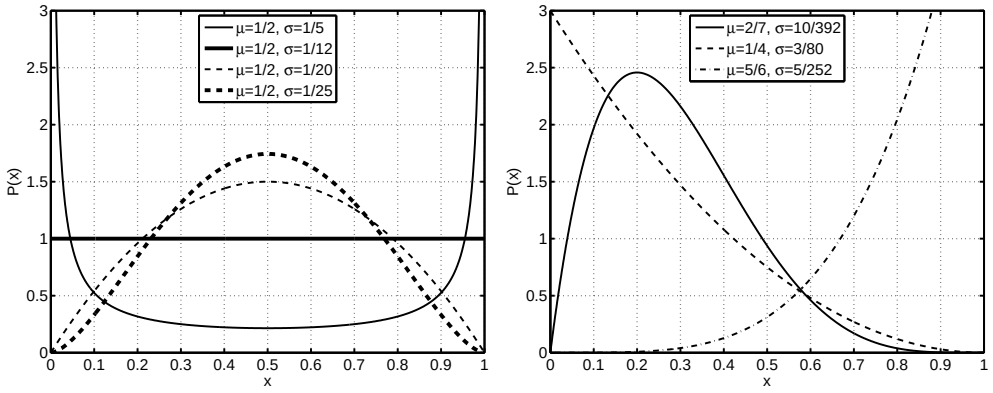

FIGURE 1. Results of a β distribution for x, for different means, $\mu(x)$ and variances of x, $\sigma(x)$. Left, symmetric modes, $\mu(x) = 1/2$, right non-symmetric modes, $\mu(x) \neq 1/2$.

number is a measure for the Kolmogorov eddy size compared to the thermal flame thickness $l_L = \Delta T/max(|\nabla T|)$. The cases are specified in Tables 2 and 3. For methane an equivalence ratio of $\phi = 0.7$ was taken and for hydrogen we had $\phi = 0.4$. The definitions of characteristic Reynolds, Karlovitz and Damköhler numbers are respectively

$$Re_L = \frac{u'l}{s_L l_L}, \qquad Ka_L = \left(\frac{u'^3 l_L}{s_L^3 l}\right)^{1/2} \qquad \text{and} \qquad Da_L = \frac{s_L l}{u' l_L}. \tag{3.1}$$

Turbulence was generated in an elongated box of size $L \times L \times 8L$. In case of the two lowest Karlovitz numbers and with methane as a fuel, the box is reduced and we only have a length of $4L$ in these cases. The integral scale of the turbulence was $l = L/10$. Lateral boundary conditions were taken to be periodic. The bottom wall was defined as an adiabatic free slip fixed wall and there is an outflow at the top. A forcing term in the momentum equations was used to initialize and maintain the turbulent background flow. Note that in the description of the hydrogen case, effective Ka, Da and flame thickness are given as well. This has to do with the fact that the laminar 1D hydrogen flame is unstable. So even without applying turbulence it will generate cellular structures, see also Bastiaans and Vreman (2012). This case, without turbulence, was run to determine the effective numbers. The appearing structures were characterized by an effective thickness and an effective propagation velocity. This latter value was determined by the propagation velocity at locations where the nominal equivalence ratio occurs ($\phi = 0.4$).

The (unpublished) DNS data analyzed here was generated with the low Mach number code, LMC, by Day & Bell (2000). LMC is second order accurate in space and time, and for this study incorporates detailed models for chemical kinetics and mixture-averaged species transport, as specified in the GRIMech 3.0. Note that all argon and nitrogen-containing species except N_2, and the reactions involving them, were removed for the methane runs. For the hydrogen runs, the mechanism of Li et al. (2004) was applied. The procedures used for problem setup and data extraction follow closely those discussed in Aspden et al. (2011). Adaptive mesh refinement was used to focus computational effort near the dynamic flame surface, achieving an effective fine grid resolution of $1024 \times 1024 \times 8192$. For the current analysis, regions containing locally refined data were averaged (numerically conserving species mass and energy) to the uniform base grid ($256 \times 256 \times 2048$) in order to maintain consistent statistics.

Case	Meth01	Meth04	Meth12	Meth36
Ka number	1.0	4.0	12.0	36.1
Da number	2.52	1.0	0.481	0.231
Integral length scale	0.00264	0.00264	0.00264	0.00264
RMS velocity	0.299	0.754	1.570	3.27

TABLE 2. Different cases of methane combustion at $\phi = 0.7$, $S_l = 0.1886$ m/s a flame thickness of $\delta = 0.00066$ m. Domain size $L \times L \times 8L$, with $L = 2.64$ cm, at a grid of $1024^2 \times 8196$ and half the lengths for the two lower Ka cases.

Case	Hydr01	Hydr04	Hydr12	Hydr36
Ka number	4.0	15.9	47.7	143.2
$\mathrm{Ka_{eff}}$	1.0	4.0	12.0	36.1
Da number	0.72	0.28	0.14	0.07
$\mathrm{Da_{eff}}$	2.52	1.0	0.481	0.231
Integral length scale	0.00164	0.00164	0.00164	0.00164
RMS velocity	0.7524	1.896	3.946	8.216

TABLE 3. Different cases of hydrogen combustion at $\phi = 0.4$, $S_l = 0.224$ m/s and a flame thickness of $\delta = 0.000682$ m. The effective burning velocity with 3D freedom but no turbulence (so including unstable behavior for the current domain) is $S_l = 0.474$ with a thickness of $\delta = 0.000410$ m. Domain size $L \times L \times 8L$, with $L = 1.64$ cm at a grid of $1024^2 \times 8196$.

4. Data

Similar to the cases discussed in Aspden et al (2011), the DNS runs were integrated numerically in time until a quasi-steady flame brush was established. The mean flame propagation is downward in the negative z direction, and in all cases the flame brush was still sufficiently far away from the lower boundary. Cross-sections (in the x-z plane) of representative snapshots from the solutions are shown in Figures 2 and 3. The figures show the fuel consumption rate, the temperature and the mass density for realizations at increasing Karlovitz numbers. Note that only a subdomain centered on the flame surface is shown for the taller cases. We see that the complexity of the flame surface, including the local curvature, increases dramatically with Karlovitz number in both cases, as expected. Furthermore, it is apparent that the temperature and density are nearly complements of each other, reflecting the constant pressure assumption for these low Mach number flows. Furthermore, the fuel consumption profiles in the hydrogen cases show significant variability along the flame interface characteristic of structures typically attributed to preferential diffusion effects. In the low Karlovitz cases, the flame structures appear to be genuinely disconnected. Interestingly, at higher Karlovitz numbers, the hydrogen flames appear to form relatively flat elongated structures that consume fuel on both sides – i.e., tongues of fuel are surrounded by hot products.

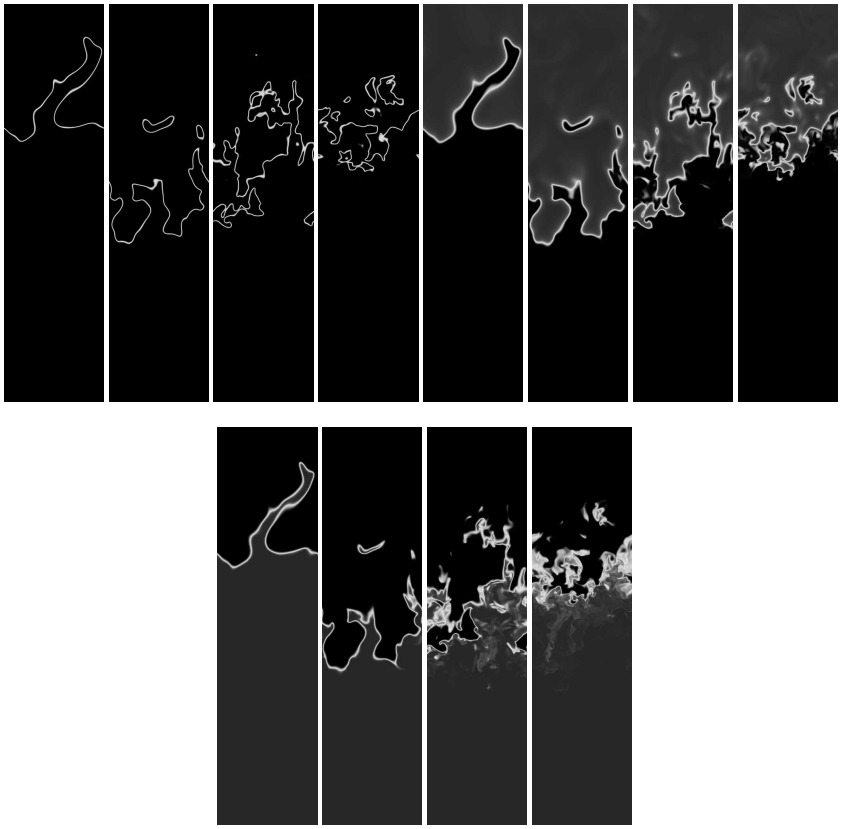

FIGURE 2. Two-dimensional plots of the source term (left) and temperature (right) for methane combustion at $\phi = 0.7$ in the ranges of [0, 62] $kg\,m^{-3}\,s^{-1}$ and [298, 1870] K, and density (bottom) in the range of [0.183, 1.144] $kg\,m^{-3}$. The sets of 4 plots indicate Ka=1,4, 12 and 36 from left to right. Here the pictures are drawn to scale with a factor of 2 (the actual domain is 2 times as big).

Using these flame simulations, we gather statistics in planes normal to the mean propagation, i.e. mean statistics in the x-y planes are assumed to be homogeneous and isotropic. For the methane flames, the progress variable is defined by the mass fraction of carbon-dioxide, Y_{CO_2}; for the hydrogen flames, the mass fraction of water, Y_{H_2O}, is taken. These values are scaled with the adiabatic value that can be found from the calculation of stationary free adiabatic laminar premixed flames with CHEM1D, applying the same kinetic scheme.

The mean and variance of the progress variable as function of z are calculated for all realizations considered and are given in Figures 4 and 5. In Figure 4 the first two results are on the shorter grid; therefore, the slopes of the mean values appear to be relatively low. In general the slopes of the mean progress variables are not sensitive to the Karlovitz number but are sensitive to the difference in fuel. Traveling in flame brush direction, small dips can be observed after reaching the maximum values of the mean progress variable. This means that pockets of lowered (or unburned) progress stay behind the main initial flame front. For the hydrogen case the flame brush thickness is approximately half of the value that can be observed for the methane cases. A similar conclusion can be drawn for the variances.

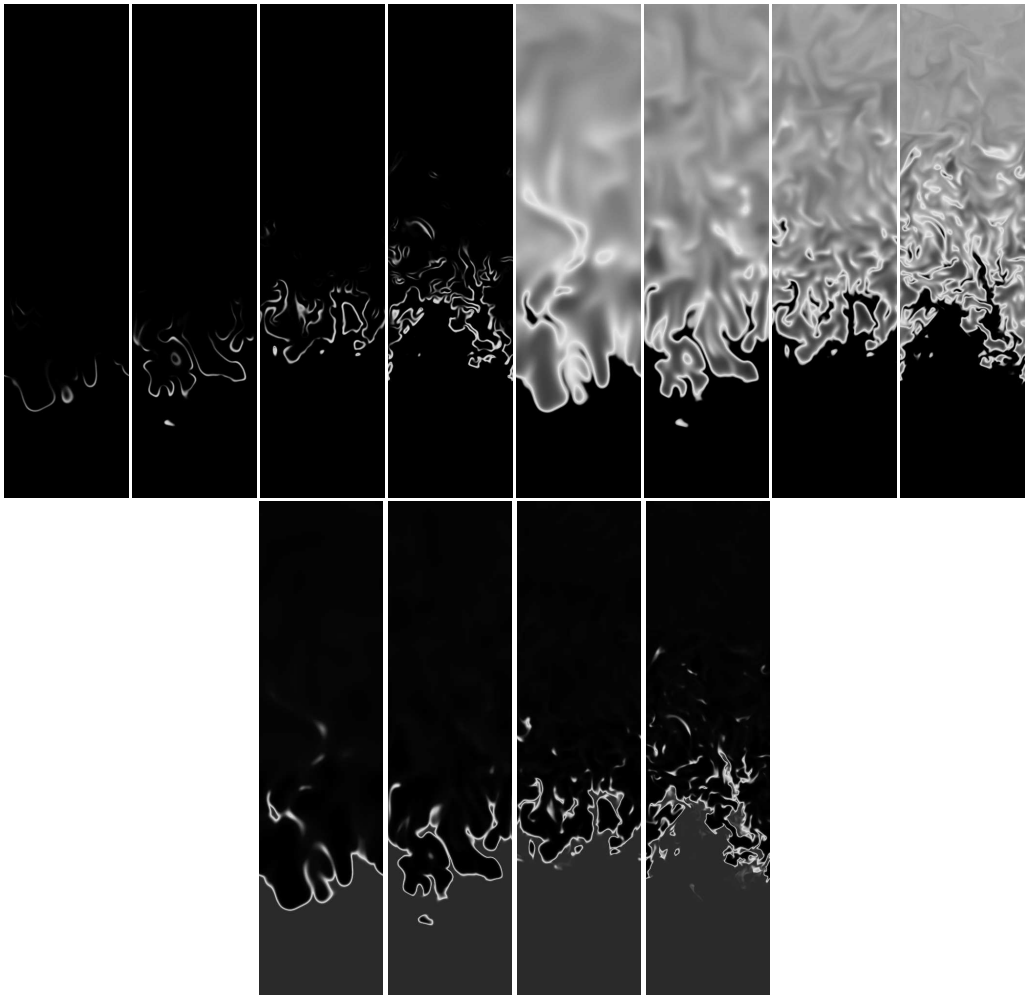

FIGURE 3. Two-dimensional plots of source term (left) and temperature (right) for the hydrogen combustion at $\phi = 0.4$ in the ranges of [0, 90] $kg\ m^{-3}\ s^{-1}$ and [298, 1770] K. Bottom set indicates density in the range of [0.178, 1.033] $kg\,m^{-3}$. Only half of the domain is shown since the combustion has not entered the lower half. The sets of 4 plots indicate Ka=1,4, 12 and 36 from left to right. Here the pictures are drawn to scale.

5. PDF analysis

An analyses of the statistics of the progress variable in horizontal, or z-planes, is carried out for given instants in time. The data is defined on an equidistant mesh so all data count equally. First we evaluate the actual PDFs of the occurrence of a certain value of the progress variable. After this we will reproduce the same information but this time on the basis of a β-PDF evaluated by the mean and variances of the observed progress variables as given in Figures 4 and 5. For this fitting procedure we consider each z plane separately. In each plane, all 256×256 observations of the progress variable are collected in 128 bins. As an aid to visually filter away bimodal behavior (due to the large number of observations in the first and last bins, at 0 and 1), we display the 10log of the probability. In Figure 6 the result is shown for the methane cases. On the y-axis we

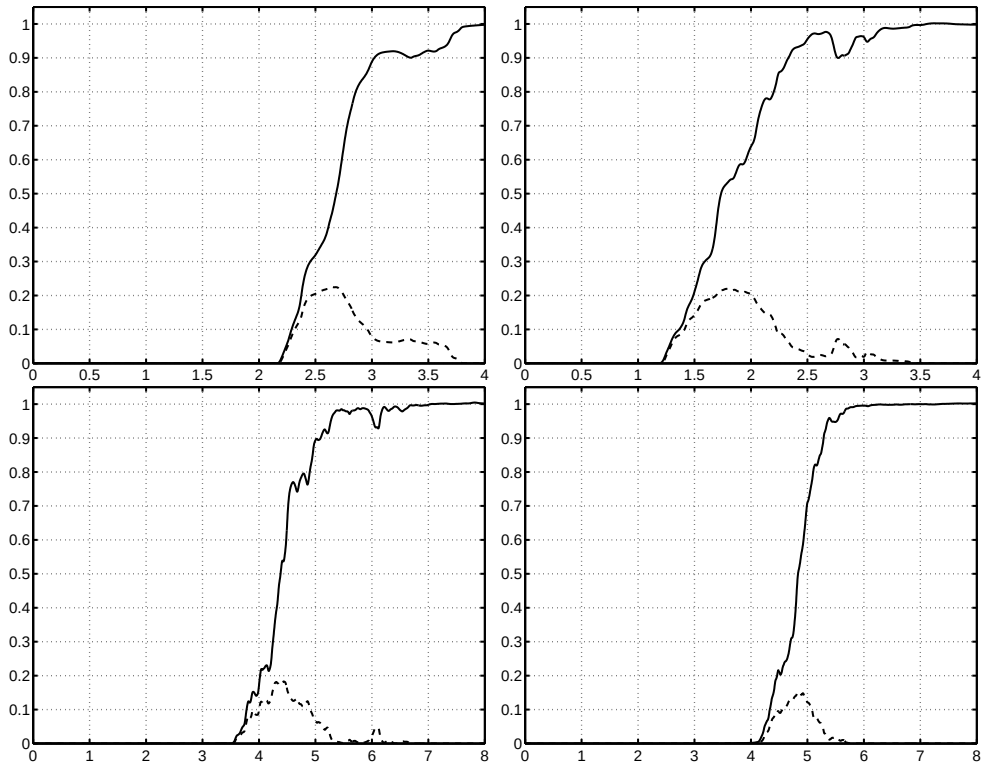

FIGURE 4. Mean (solid) and variance (dashed) of the progress variable as function of height z of the methane cases. Top left to bottom right is at increasing Ka. Note the different z scales at the lowest two Ka numbers and the highest two at the bottom.

have the downstream location and on the x-axis the value of the progress variable. The color-data are the probability densities for observing the associated progress variable. We limited the color-values corresponding to having only 1 observation in a bin, resulting in $10\log(1/128/2) = -2.4$. The maximum is set to having all observations in a single bin $10\log(128) = 2.1$. This makes all the results comparable.

The methane cases exhibit a clear bimodal distribution. For higher Karlovitz numbers intermediate values of the progress variable occur a little more, but this is marginal. However the effect of this must not be underestimated as it is in this region where the source term of the progress variable attains its maximum value. Furthermore one can see that the PDF recovered by the assumed β function is very similar to the observed PDF.

For the hydrogen data, as depicted in Figure 7, we see a slightly different behavior. Looking in the downstream direction, the unburnt state is left more rapid and there are more observations of intermediate values of the progress variable. Furthermore the results for the β-function PDF are quite dramatic. At several z locations no valid outcome was attained. That is, the β-PDF model seems to not recover the behavior of this measure of progress variable.

6. Discussion

For the methane flame cases, the observed fluctuation distributions were fit quite well by the β-PDF forms. We conclude that this confirms the utility of simple models based on

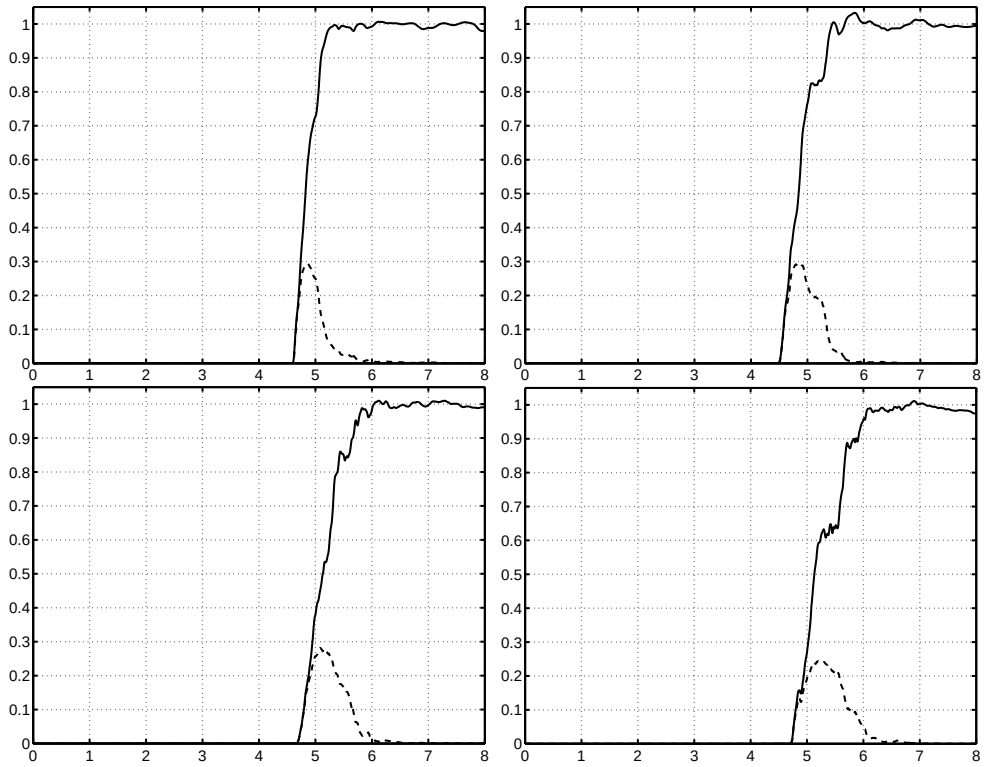

FIGURE 5. Mean (solid) and variance (dashed) of the progress variable as function of height z for the hydrogen cases. Top left to bottom right pictures are associated with increasing Ka=1, 4, 12, 36.

these fits, at least in the absence of preferential transport. For the lean hydrogen flames, we find that the parameterization fails to represent the observed behavior. However, we contend that the problem appears to be fundamental, and not likely remedied through an alternative choice of basis functions. The one-dimensional measure of progress we used, one that is a standard choice in simple flames, is seen to attain local values exceeding unity by a significant amount; even mean values of the progress value lay outside the valid range. Additionally, the failure of the model is not isolated to the extremes of the distribution, but rather throughout the flame brush. We conclude that the notion of "reaction progress" needs to be revisited and, perhaps, generalized for lean hydrogen before a presumed PDF approach can be meaningfully applied. We also note that since practical fuels will span a range of mixtures and equivalence ratios, and practical devices will operate under a range of conditions, it is likely that the conclusions here have a more general relevance.

7. Conclusions

In the current brief we studied whether simple assumed sub-resolved statistics can be used for the closure of the chemical source term for different fuels and Karlovitz numbers. To that end realizations of DNS computations with detailed chemistry and transport were analyzed. The fuels were methane at equivalence ratio of 0.7 and hydrogen at equivalence

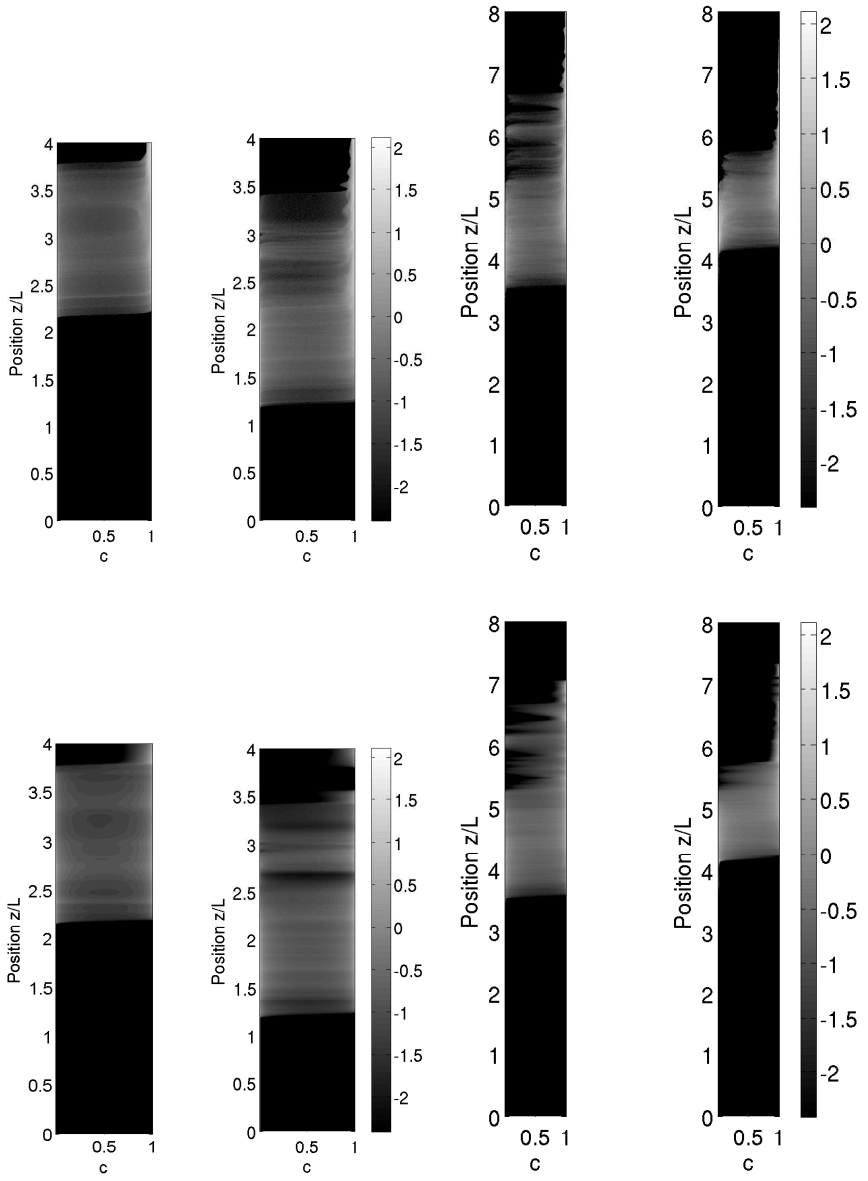

FIGURE 6. Actual and assumed β (based on actual mean and variance) probability density functions for scaled CO_2 occurrence for homogeneous $x-y$ planes as a function of z-location for methane cases. Top row: actual methane PDFs; lower row: the same but then for the model (β) PDFs. Left to right figures are respectively Ka=1, 4, 12 and 36.

ratio of 0.4. The Karlovitz numbers were taken at a relative large level of Ka =1, 4, 12 and 36.

It appeared that a β-function PDF for the closure of the subgrid chemical source term could perform well for methane combustion cases but not for hydrogen. In the hydrogen case it was observed that the water concentration, which was taken as a progress variable,

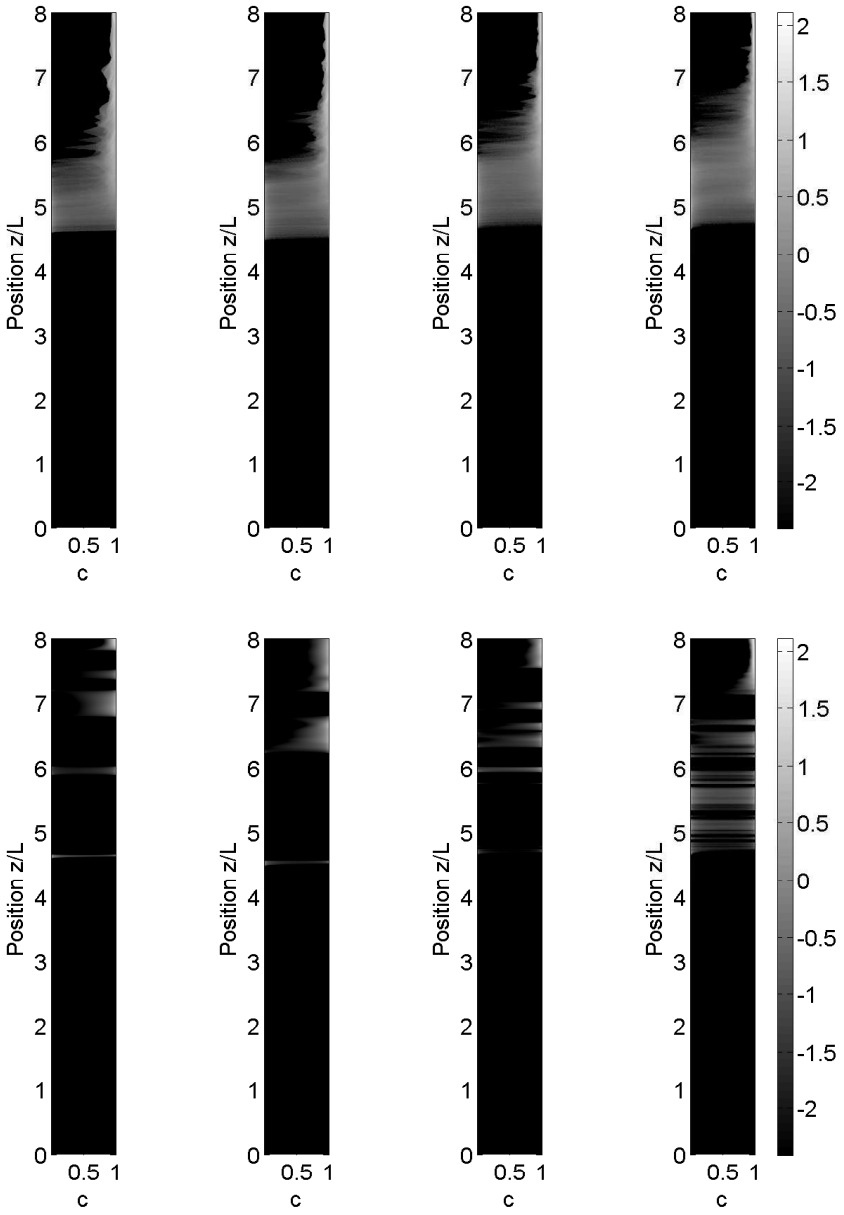

FIGURE 7. Actual and assumed β (based on actual mean and variance) probability density functions for scaled H_2O occurrence for homogeneous $x-y$ planes as a function of z-location for hydrogen cases. Top row: actual hydrogen PDFs; lower row: the same but then for the model (β) PDFs. Left to right figures are respectively Ka=1, 4, 12 and 36.

was exceeding its adiabatic value in many locations by up to 50%. While this also occurred in the methane case (where the progress variable was taken to be carbon dioxide), the adiabatic value was exceeded by less then 10%. This can be attributed to stretch and curvature events, and for the hydrogen cases to preferential diffusion. Furthermore a

typical behavior is observed for hydrogen at high Ka numbers, where elongated burning structures appear.

It is clear that the PDF for turbulent hydrogen combustion requires a different parameterization and perhaps may even be multidimensional. Thus we conclude that LES simulations of lean premixed hydrogen combustion should be suspect if based on assumed PDF modeling with a single parameter.

Acknowledgements

This research used resources of the Oak Ridge Leadership Computing Facility at the Oak Ridge National Laboratory, which is supported by the Office of Science of the U.S. Department of Energy under Contract No. DE-AC05-00OR22725. Support from CTR for appointing Rob Bastiaans as a visiting professor is gratefully acknowledged.

REFERENCES

Aspden, A.J., Day, M.S. & Bell, J.B., 2011, Turbulence-flame interactions in lean premixed hydrogen: transition to the distributed flame regime, *J. Fluid. Mech.*, **680**, 287–320.

Bastiaans, R.J.M. & Vreman A.V., 2012, Numerical simulation of instabilities in lean premixed hydrogen combustion, *Int. J. Num. Meth. Heat & Fluid Flow*, **22** (1), 112–128.

CHEM1D, 2007, A package for the simulation of one dimensional flames. Eindhoven University of Technology, Version 3.0, http://www.combustion.tue.nl.

Cook, A.W. and Riley, 2004, J.J., A subgrid model for equilibrium chemistry in turbulent flows, *Phys. Fluids*, **6**,2868-2870.

Day, M.S. & Bell, J.B., 2000, Numerical simulation of laminar reacting flows with complex chemistry,*Comb. Theory & Modelling*, **4**(4), 535-556.

Gicquel, O., Darabiha, N. and Thevenin, D., 2000, Laminar premixed hydrogen/air counter flow flame simulations using flame propagation of ILDM with preferential diffusion. *Proc. Combust. Inst.*, **28**, 1901–1908.

Li, J., Zhao, Z., Kazakov, A. and Dryer, F. L., 2004, An updated comprehensive kinetic model of hydrogen combustion, *Int. J. of Chemical Kinetics*, **36**, 10, 566–575.

GRIMech3.0, Smith, G.P., Golden, D.M., Frenklach, M., Moriarty, N.W., Eiteneer, B., Goldenberg, M., Bowman, C.T., Hanson, R.K., Song, S., Gardiner Jr., W.C., Lissianski, V.V. and Qin, Z.. http://www.me.berkeley.edu/gri_mech/

van Oijen, J.A. & de Goey, L.P.H., 2000, Modelling of premixed laminar flames using flamelet-generated manifolds, *Combust. Sci. and Tech.*, **161**, 113-137.

Peters, N., 2000, Turbulent Combustion, Cambridge University Press.

de Swart, J.A.M., Bastiaans, R.J.M., van Oijen, J.A., de Goey, L.P.H., & Cant, R.S., 2010, Inclusion of preferential diffusion in simulations of premixed combustion of hydrogen/methane mixtures with flamelet generated manifolds. *Flow Turb. Comb.*, **85** 3-4, 473–511.

Vreman, A.W., van Oijen, J.A., de Goey, L.P.H. and Bastiaans, R.J.M., 2009, Subgrid scale modeling in large eddy simulation of turbulent combustion using premixed flamelet chemistry. *Flow Turb. Comb.*, **82**, 511–535.